## Minimally invasive sequential analyses of questioned paintings: Six experiments in art authentication

Murphy G. Brasuel, Amanda C. Bowman, Conor J. K. Blanchett, Nathan W. Bower\*

Chemistry and Biochemistry, Colorado College. Colorado Springs, CO 80903, USA \*Corresponding author: <a href="mailto:nbower@coloradocollege.edu">nbower@coloradocollege.edu</a>

Abstract: Non-destructive and micro-destructive analyses play an important role in determining the authenticity of art works. These include determination of the composition and date of manufacture. Similar analyses are used for a range of forensic problems. However, the importance of "do no harm" to the object places a significant additional constraint beyond simply preserving evidence for future analyses. The rise in art theft and fraud cases recently and the need for rapid, non-destructive analyses to meet statute of limitations restrictions underscores the need for greater awareness and training in the analysis of works of art that may be forgeries or worth millions of dollars. A sequence of laboratories that address art authentication questions are shown in an order that minimizes sample usage and emphasizes the thought processes used in crime scene reconstruction. We outline six undergraduate laboratory exercises using a case study that includes novel wood and paint dating methods. We compare some simple methods to state-of-the-art instrumental analyses typically used in legal cases, using these to cross-validate the conclusions.

Keywords: art authentication, paint cross-section, Py-GC-MS, reflectance spectroscopy, XRF

#### Introduction

According to the US Department of Justice, art crime is the third highest-grossing criminal trade in the world, right after drugs and weapons (1-2). Reports of cultural property theft through illicit excavations in the Americas doubled during the recent pandemic, while authentication services decreased (3). Art fraud, though smaller in value than theft, is larger in quantity. The Fine Art Expert Institute (FAEI) in Geneva discovered 70 – 80% of art they test is not by the claimed artist (4).

Victims are responsible for seeking legal recourse if they discover an artwork is fake or stolen. The Uniform Commercial Code (U.C.C.) statute of limitations for a suit against the seller is only four years. Most victims do not discover the problem until too late. For financial gain or to avoid embarrassment, the victim may try to pass the loss to a new buyer, compounding the crime. Fraud and breach of contract or warranty are covered by state and civil law while wire (internet) and mail fraud, tax evasion, and money laundering are covered by federal law (5).

Forensic science inherently requires an integration of natural and social sciences. Multi-disciplinary puzzles that incorporate creativity, logical progression, and critical thinking are educationally necessary to develop the skills required by the discipline. An excellent paper by Michelle Miranda (6) describes the parallel skills involved in forensic science and art "connoisseurship" vital to developing a narrative during crime scene reconstructions. These include observation, inference, analytical techniques (chemical and physical), experience (contextual awareness and historical perspective), and

communication. Miranda provides a detailed history of how the two disciplines developed by borrowing from each other (e.g., Locard and Morelli). She concludes with some perspectives from educational philosophy that underscore the importance of art when educating forensic scientists. A similar emphasis on the importance of context and historical perspectives may be seen in Quarino and Brettell (7). Many useful laboratory exercises at the intersection of art and forensic science are in the literature (8-12).

In this study, a questioned copy of the painting *The* Man with the Golden Helmet (hereafter MGH-Copy) is used as a unifying case for six laboratory exercises suitable for undergraduate instrumental analysis or forensic science courses with "art authentication" modules. A sequence of experiments is described that maximizes information while minimizing damage. Time and money are constraints that must be balanced against jumping to a conclusion when there are other explanations. Novel, inexpensive laboratory methods for dating wood, identifying paint binders, and mapping zinc oxide in paint cross-sections are presented and compared to traditional methods. Method and object substitutions can be made according to available resources and student background. However, a logical sequence of analyses with cross-validation of results are as crucial here as they are in any crime scene analysis.

#### **Background of the artwork**

The Man with the Golden Helmet (hereafter MGH-Original, unknown artist, ca. 1650–1660, 67.5 × 50.7 cm)

is an oil painting on canvas housed at the Gemäldegalerie, Staatliche Museen zu Berlin, Berlin (no. 811A). *The Rembrandt Database* (13) provides a detailed provenance. It was attributed to Rembrandt van Rijn (1606–1669) when first displayed in 1898. However, it was reattributed to a pupil of Rembrandt in 1986. White lead, smalt, umber, and a copper pigment have been identified in the original. Earlier restorations were done in 1897 and ca. 1796. The painting was cut from 73.2 × 59.6 cm to its current size, cropping the helmet's feathers.

The MGH-Copy (68  $\times$  51 cm) was purchased ca. 2010 in Argentina. The owner hoped this was the original Rembrandt (worth millions of dollars) or a work by one of his students (worth hundreds of thousands). Photographs of the front (**FIGURE 1**) and back, a sliver of wood from the supporting cradle, and a few paint chips were supplied by the owner. The man in the MGH-Copy is angled differently than in the MGH-Original (13) and the MGH-Copy is on a wood panel rather than a canvas. Areas of significant paint loss are visible along cracks, and the stabilizing cradle has lost a crosspiece (**FIGURE 2**).

## Hazards and Safety Precautions

Though only a few drops of reagents are used in Exercises 3, 4, 5, and 6, acids and bases can cause chemical burns, and dyes, solvents and index of refraction liquids are carcinogenic and/or acute toxins if ingested. Nitrile gloves and safety goggles should be worn during handling. Safety goggles should also be worn when using ultraviolet (UV) light (Exercises 1 and 2). Finally, open flames and hot glass in Exercise 6 are a burn hazard. All reagents and their safety data are available from Sigma-Aldrich.



FIGURE 1 MGH-Copy, oil on oak panel, date and artist are unknown.

2023 Journal of Forensic Science Education

#### Sequential analysis scheme

Given limited access and samples, a logical sequence of analyses must be chosen that maximizes the information from imperfect samples (**TABLE 1**). Three dark brown paint chips  $(0.2-0.3 \text{ mm} \text{ thick}, 2-4 \text{ mm}^2, 1-2 \text{ mg} \text{ each})$  and a wood sliver were ultimately used. A single 2 mg chip, split into smaller pieces, could be used for all the analyses with some loss of sensitivity. Standard methods (14, 15) were used for the instrumental procedures not detailed here. Many are applicable to fake artifacts, coins, and documents as well as painted art (16).

Note: it is not necessary that samples given to students come from fine art. Paint chips from a 100-year-old painted wall can be paired with images of "questioned" art. Photos with four 4 mm² chips are usually adequate for up to 16 students. Larger classes might analyze chips from different objects. If art that might be valuable is to be sampled, we encourage consulting an art conservator.



**FIGURE 2** Wood cradle (bottom) and panel (top) where a crosspiece was lost. Stain bleeding (lower left) and residual glue spots (upper right) are visible.

#### Methods

#### **Non-Destructive Methods**

Exercise 1: Preliminary examination and estimation of wood age

Exercise 1 is primarily a dry lab. We have treated it as a library and/or in-class lab with internet access. Exercise 1 using a color chart does not require any equipment. A reflectance spectrometer is optional but useful if artwork is physically available for analysis.

Any documentation related to the origin and history of the work should be reviewed. If the artwork is available, an inspection using raking visible, ultraviolet, and near infrared light should be made. These lights can detect paint adhesion issues (raking light), areas of restoration (old varnish fluoresces more than new under UV light), and underdrawings (near IR). Odors from any recent work and inconsistencies from wrong-era tool markings should be recorded.

**TABLE 1** Sequence of analyses used to minimize sample consumption and maximize information extracted.

## I. Preliminary examination of the painting (non-destructive):

- 1. Provenience [Provides the painting's history; ownership; authentication]
- 2. Artistic style, brush strokes, comparison to known paintings [Differentiates artists; expert opinion/authentication]
- 3. Paint: appearance, varnish, sniff test, state of preservation, paint loss, chip location [Age, paint type]
- 4. Frame: appearance, age, style, tool marks, wood(s), state of preservation [Age]
- 5. Back of painting: mounting type, appearance, labels, signatures, dates, tool marks, wood(s), oxidation color [Age]

## II. Alternative light sources (ALS) (non-destructive):

- 6. Visual appearance/color(s), raking light examination [Shows brush strokes, damage areas]
- 7. UV fluorescence [May identify whites, as TiO<sub>2</sub> absorbs, others fluoresce in different colors; varnish age]
- 8. Near-IR absorbance [Differentiates blacks]
- 9. Magnetic susceptibility [Measure of Fe content and valence, differentiates blacks]

## III. Spectral analyses (mostly non-destructive):

- 10. VIS [Differentiates metamers used during restoration; identifies some pigments]
- 11. IR [Identifies varnish and binders, but also differentiates minerals and pigments]
- 12. XRF [Identifies major and minor element analysis]
- 13. Raman [TiO<sub>2</sub> very strong signal; detects oils versus varnish; some minerals and pigments]
- 14. XRD [Identifies major minerals like the ground and some pigments; crystallinity may identify synthetics]
- 19. ICP-OES or AA [Destructive: use the residue from Py-GC-MS to obtain trace element analyses]

## IV. Microscopy (destructive, but gives the most information from the smallest sample):

- 15. Cross-section analyses [Binding media type by reagent staining; observe paint layer structure, particle sizes
- 16. PLM [Particle sizes; identify inorganic/organic pigments; microfossils; canvas fibers; wood type]
- 17. SEM-EDX [Very fine particle sizes; paint structure; nannofossils; elemental analyses of individual particles]

## V. Chromatographic analyses (destructive):

- 18. GC-MS and Py-GC-MS [Identifies binder types, source, and age; identifies some organic pigments]
- 20. LC-MS [Useful if organic pigments/dyes are present; better for thermally labile compounds than GC-MS]

In addition to damage from insects and "distress" from handling over time, wood in contact with air, heat, humidity and/or sunlight changes color, primarily through degradation of extractives and lignins. This degradation increases blue light absorption. However, photobleaching and blue-green fluorescence of degradation products makes use of blue wavelengths problematic. Age estimates are made from untreated wood that has been protected from light and held in a constant (e.g., indoor) environment. Red light reflectance increases over time as reddish quinones are formed from oxidation of lignins (17-18).

For this study, 700 nm reflectance from unfinished, oxidized, light-colored woods (interior surfaces of dated oak and pine furniture) were measured with a Xenon flash lamp (D65 illuminant, 10° observer at a 45° angle) using a hand-held reflectance spectrometer (Avantes AvaMouse, Avantes, Lafayette, CO). Multiple measurements were made to assure a representative analysis. RGB values were calculated from the CIELAB data.

The natural log of R from RGB is linear with time on the x-axis. (Time is the independent or control variable

for this pseudo first order reaction.) Dates were obtained by subtracting the age (years ago) from the current date.

Other reflectance spectrometers may have different calibrations and dated wood samples may not be available. However, RGB pixel data from photographs can be used instead. Photos of the MGH-Copy wood cradle were opened in Microsoft Paint. Areas with >10,000 pixels that averaged the light and dark wood grain were saved as sub-files. RGB data were obtained using the National Institutes of Health (NIH) ImageJ, downloaded freeware (>Plugins, >Analyze, >RGB-Measure). Uncorrected, online photos of unfinished, oxidized wood panel paintings in museums and art auctions dated 1650 to 2010 were used for calibration.

D65 refers to diffuse, midday light (6500K color temperature). Phone LED flashes are direct light at 5500K. Indoor color correction may be needed using a matte white tile next to the wood to be dated. If the tile is also measured using D65 10° conditions, multiplying the wood's mean R by the tile's D65/flash ratio can give a rough correction. Color cards may be used to adjust camera color balances, but the online photo calibration

data here was used "as is". Color dating may be done very simply with **FIGURE 3a**.

For a (destructive) radiocarbon date to compare to the proximate dating based on red color development, an unstained wood sample from the cradle backing was submitted to Geochron Laboratories (Chelmsford, MA) for a <sup>13</sup>C-corrected <sup>14</sup>C date. They first treated the wood with hot dilute HCl to remove carbonates, then 0.1 M NaOH to remove organic contaminants, and again with dilute HCl. After washing and drying, the sample was combusted to give CO<sub>2</sub> for dating by accelerator mass spectrometry. Note: radiometric dating is usually done by specialist laboratories, not by forensic scientists or art conservators. However, the ability to interpret the basic decay equation at the first-year undergraduate level and the <sup>13</sup>C corrections at an advanced level are useful skills.

## Exercise 2: Composition analyses from spectra

Many spectral methods are taught in undergraduate courses. Students enjoy looking for evidence of forgeries with these methods. Comparing and contrasting ambiguous evidence from different methods gets them thinking more deeply about quality control and method limitations. If teams of two or three students use different methods and then present and defend their analyses in class discussions, useful forensic skills are developed.

Top (varnish) and bottom (ground) surfaces of "as provided" paint chips were analyzed using a UV lamp (Mineralight UVGL-25, Thomas Scientific, Swedesboro, NJ); attenuated total reflectance-FTIR using a Bruker (Billerica, MA) Alpha 1 mm² window diamond cell ATR-FTIR; X-ray diffraction using a PANalytical (Malvern, UK) X'pert Pro XRD; and Raman using a Renshaw (West Dundee, IL) inVia Raman with a Leica optical microscope with 532 and 785 nm lasers and WiRE 5.5 software. These gave four methods of analysis for each surface (a total of eight comparisons for discussion with up to 24 students in groups of three). When groups worked simultaneously on several chips, all the analyses were done in one lab period. With more time, teams rotated to different instruments.

Element maps and X-ray spectra were created with a Zeiss (Jena, Germany) EVO MA 15 scanning electron microscope—energy dispersive X-ray spectrometer (SEM-EDS) using 50 Pa and an uncoated chip edge mounted on sticky carbon on a stub. Analyses were also done using a JEOL JSM-6390LV and Oxford 7582 EDS by senior students to provide non-destructive analyses to compare to cross-section mapping using stains (see below). Usually, classes get these results in the form of an "expert report".

#### **Destructive Methods**

#### Exercise 3A: Cross-section paint binder mapping

Even quick-setting resins are best left to harden for many hours, making this a two or three period exercise unless the instructor prepares the samples beforehand. Multiple chips may be cast concurrently in 1 cm<sup>3</sup> silicone ice cube trays. Very small chips can be hard to find unless a small label or mark is put next to the chip before the second layer of resin is poured. The resin cube is sanded with progressively finer sandpaper at 90° to the casting layer to expose a cross-section. To save time, this step is usually done for mid- to lower-level undergraduates.

A  $\leq$ 1 mg MGH-Copy paint chip was immersed in epoxy, dried, and a cross-section was exposed for staining by cutting and sanding (>8000 grit). Because the paint film appeared porous, epoxy was chosen over polyester resin. Though polyester resin is usually preferable for optical and fluorescence staining, polyester penetrates porous samples (19), interfering with micro-Raman, etc. studies that might also be conducted on the cross-section.

Following the method of Wolbers and Landrey (20). binding media (carbohydrates, proteins, and oils) were elucidated using fluorochrome stains: triphenyl triazolium chloride (4% in dry methanol), fluorescein isothiocyanate (0.06% FITC in acetone), and Rhodamine B (0.02% in ethanol), respectively. These were viewed with a Zeiss Axioskop upright fluorescence microscope with 50W Hg lamp excitation, and Chroma<sup>TM</sup> and Zeiss filter cubes optimized for these tests. For TTC a Chroma<sup>TM</sup> custom filter cube with a HQ410/30 excitation filter, Q430lp dichroic mirror, and a HQ455 LP (low pass) emission filter was used. For FITC a Chroma TM custom filter cube with a D510/20 excitation filter, 530dclp dichroic mirror, and a HQ545 LP emission filter was used. For Rhodamine B Zeiss<sup>TM</sup> Filter Set no. 15 with a BP (band-pass) 546/12 excitation filter, FT 580 dichroic mirror, and a low pass 590 emission filter were used. Binding media may also be identified using spot tests (21). While the stains usually are applied sequentially in the above order to minimize sample use, multiple chips may be treated in parallel at different stations for Exercise 3A and 3B to shorten lab time.

### Exercise 3B: Element mapping with stains

Because stains and dyes from cross-section analyses are often persistent, the cross-section was sanded and polished again. The cross-section was stained with acidified potassium iodide (KI). It forms a yellow precipitate with lead white (2PbCO<sub>3</sub>·Pb(OH)<sub>2</sub>) (19). KI/I<sub>2</sub> (0.1g/0.05g in 1 mL H<sub>2</sub>O) was used to map starch. After

surface cleaning, zinc white (ZnO) was mapped as a red stain in the chip with 0.01% dithizone in dichloromethane (CH<sub>2</sub>Cl<sub>2</sub>, a carcinogen) using a 30x binocular microscope. Photographs of the cross-section were taken through the microscope eyepiece with a Pixel 4 phone. This method is based on the spot test of Plesters (22). To our knowledge, its use for mapping has not appeared in the literature.

#### Exercise 4: Polarized light microscopy and microfossils

A paint chip (2 mg) was placed in a round-bottomed, glass vial with 2.0 mL of 1:1 dry methanol (CH<sub>3</sub>OH) and CH<sub>2</sub>Cl<sub>2</sub>. This was capped (PTFE liner) and left overnight. The paint chip was pulverized with light pressure from a glass rod and dispersed without sonication. The suspension of particles was split into two vials, one for polarized light microscopy (PLM) and microfossil analysis and one for fatty acid methyl ester (FAME) analysis (*Exercise 5*).

The particles in the first vial were washed with dry methanol and mixed with fresh methanol for microscopy using a Leitz LaborLux 11 POL S microscope. The slides used for PLM were also used for nannofossil analyses. Smear slides were prepared by pipetting and spreading the particle-methanol suspension on slides. After the methanol evaporated, dry particle smears were covered with a drop of immersion oil ( $n_D = 1.515$  or 1.660) and a thin (#0, ca. 100 µm thick) coverslip. Permanent PLM mounts may be made using Cargille Meltmount<sup>TM</sup>  $n_D =$ 1.539 and 1.662. Comparisons were made to a library of exemplar slides and PLM data (see results) provided by the instructor. Flow charts with decision trees are helpful in identifying the pigments, but complex mixtures can be time consuming to work up completely. With multiple microscopes and slides, students can be assigned light, dark, or colored particles for identification and a time limit (1–2 hour) for this exercise if PLM basics (e.g., Becke line test) are demonstrated first.

#### Exercise 5: GC-MS paint film oil date

Sample preparation for this exercise usually takes less than an hour. An autosampler is used with a GC for the analyses. Different drying oils (e.g., walnut, linseed, poppyseed) are prepared in tandem with the paint chip extracts. Printouts of the chromatograms for multiple samples are provided the next day. As the number of fatty acid methyl esters (FAMES) is limited, standards or retention times and a flame ionization detector (FID) may be used instead of a mass spectrometer for identifying the different FAMES.

FAMEs from oils in the binding media were created following the 2015 EUR-Lex method (23) for olive oils. An aliquot (0.2 mL) of 2M methanolic potassium hydroxide (0.11 g KOH/mL dry CH<sub>3</sub>OH) was added to

the 1:1 CH<sub>2</sub>Cl<sub>2</sub>:CH<sub>3</sub>OH solvent and powder in the vial. The vial was capped and shaken for 30 s. Particles were allowed to settle for 2-5 min and the supernatant was pipetted into a vial containing 0.2 g anhydrous sodium sulfate. This was shaken and allowed to settle for 5 min before transferring the supernatant to a GC-MS vial. The vial was capped and analyzed immediately or refrigerated for up to 12 hours for subsequent analysis using the same GC-MS and program used for Py-GC-MS (see below). The areas of the peaks were integrated, and the relative percent of the oleic acid (C18:1) was compared to calibration data (see results) obtained from paint samples with known dates. Note: residual particles from the FAME analysis cannot be used for PLM and microfossil studies, as acids and bases destroy the calcareous and siliceous skeletons, respectively. However, after drying, the particles may be used for elemental analyses. (See optional under Exercise 6.)

# Exercise 6: Identification of paint binders and pigments using Py-GC-MS

Because the glass-blowing technique in this exercise requires some practice and potentially limiting equipment (torches, hand pumps, and a GC-MS), this exercise is usually done by upper-level students with instrumental experience. However, Bunsen burners with glass pipets have been made to work as well (24).

Organic binders and pigments may be identified using pyrolysis-gas chromatography-mass spectrometry. Off-line pyrolysis (Py) in a Pyrex tube was done using a natural gas-oxygen torch (24). The tube was sealed with the torch while being evacuated (≤18 Torr) with a Mityvac hand pump. Distillate from the sample was formed by waving the end of the sealed tube containing a 2 mg paint chip through the flame until it charred. This was done while holding it horizontal with a wet paper towel on the cool end to condense the distillates. The tube was cut between the char and distillates. The distillates were dissolved in 1 mL CH<sub>2</sub>Cl<sub>2</sub> for analysis by GC-MS (Agilent 7890A-5975C; 30 m HP-5MS column; 250°C splitless injector; 70 eV e ion.; 50-450 amu; temperature program = 40°C for 2 min, then to 325°C at 8°C/min; He flow 1.35 mL/min). Exemplars of pigments and animal and plant binders were pyrolyzed and analyzed in the same way. These were analyzed by the undergraduates or provided as a library for comparison.

(Optional): The pyrolysis char residue in the Pyrex tube was leached with 5 mL of a 0.5 M HNO<sub>3</sub> and 1 M HCl mix and analyzed for inorganic elements with inductively coupled plasma-optical emission spectrometry (ICP-OES).

#### **Results and Discussion**

#### Non-destructive methods

Exercise 1: Preliminary examination and estimation of wood age

Provenance data for the MGH-Original is revealing, as its physical dimensions are the same as the MGH-Copy despite the original being on canvas that was cut down ca. 1800. It is unlikely that the MGH-Copy on wood panel would be cut in the same way if it were painted ca. 1650. An image of the MGH-Original was not published until 1907, though two private copies were painted earlier (13).

The raking light photograph (FIGURE 1) revealed cracks from the wood panel. It also showed a matte surface without any craquelure. Old oil paintings usually exhibit craquelure. Large flakes appeared to be peeling off the painting. This suggested instability in the ground and its attachment to the wood panel.

Under UV light, the varnished side of paint chips gave almost no fluorescence using 254 nm excitation and a greenish fluorescence with 366 nm. Aged sandarac and mastic usually are excited by both wavelengths, while aged dammar resin is excited primarily by 366 nm (25). A whitish fluorescence from the ground was consistent with gypsum (CaSO<sub>4</sub>·2H<sub>2</sub>O) and calcite (CaCO<sub>3</sub>) gesso, but without major amounts of titanium dioxide (TiO<sub>2</sub>), ZnO, or oil binder that impact the fluorescence emission. The visible light reflectance spectrum of the paint chip surfaces supported the presence of gesso and suggested the brown pigment contained ferric oxide, Fe<sub>2</sub>O<sub>3</sub> (26).

Wood exposed to air darkens over time as it oxidizes and an estimate of the time since it was last resurfaced can be obtained. This assumes no staining, cleaning, exposure to light, or protective coatings. In **FIGURE 2**, bleeding of the stain used to create the appearance of age was noted.

From comparisons to wood standards (USDA and/or Sauers & Company), the wood grain was consistent with coarse-grained white oak like that used by Rembrandt's Circle. However, the lack of  $17^{th}$  century tool marks and no signs of age (e.g., wormholes) suggested the backing was constructed or resurfaced recently. The estimated date (**FIGURE 3b**) obtained from the stained panel in the photograph of the *MGH-Copy* cradle and panel was 1808  $\pm$  25 (1s) CE. This date is false due to the stain on the wood. If the wood had not been altered, the process could have given a preliminary, non-destructive estimate of its age.

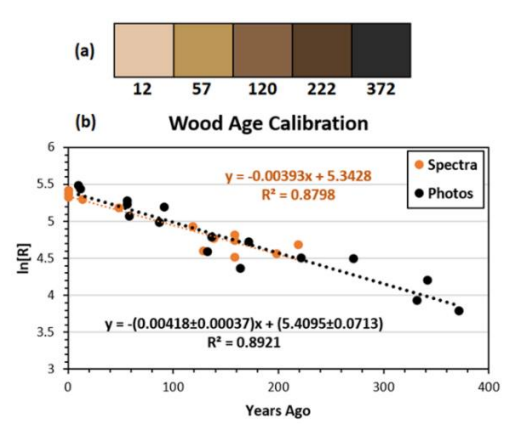


**FIGURE 3** (a) Colors from photos of five aged woods. Estimated ages may be obtained by visual color matching. (b) Wood age calibration plots from reflectance spectra at 700 nm, and from RGB digital photograph data.

Different spectrometers require calibration, but the use of RGB reflectance data and cell phone images for dating forensic evidence is a rapidly expanding field, most notably for bloodstains (27), bruises, and liver mortis (28).

The radiocarbon dating of the unstained, wood sample from the cradle backing gave an age =  $119 \pm 25$   $^{14}$ C years BP ( $^{13}$ C corrected), where the "present" is 1950 CE. The date by this method =  $1831 \pm 25$  (1s) CE. Unlike the *MGH-Copy* stained wood date of  $1808 \pm 39$  (1s) CE, this is an accurate date. It implies the wood panel and cradle may have been recycled from an earlier painting. The wood was probably stained to mimic the earlier age.

Exercise 2: Composition analyses from spectra

Non-destructive spectral analyses of the surfaces with ATR-FTIR indicated the varnish layer was dammar or sandarac resin. Dammar resin, which comes from SE Asia, was not generally available in Europe until 1827, while sandarac from Africa was available in Europe even in antiquity (29). The ATR-FTIR analysis of the ground indicated a 1:2 mix of calcite and gypsum with a small amount of an organic binder. This was supported by XRD, which revealed a mix of calcite and gypsum minerals in the ground. With less certainty because the overlying varnish inhibits the signal, XRD also detected calcite and a hydrated Fe<sub>2</sub>O<sub>3</sub> in the pigment layer.

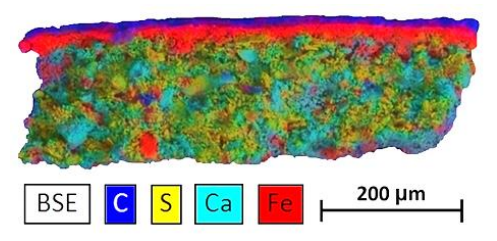


**FIGURE 4** SEM-EDS map of selected elements in an uncoated paint chip cross-section, varnish side at the top. Calcite (CaCO<sub>3</sub>) and gypsum (CaSO<sub>4</sub>·2H<sub>2</sub>O) are major components of the ground. Iron oxide (Fe<sub>2</sub>O<sub>3</sub>) is a pigment.

The SEM-EDS element maps of an uncoated paint chip cross-section detected carbon (C) in the varnish, iron (Fe) and manganese (Mn) in the pigment layers, and calcium (Ca) and sulfur (S) in the ground (FIGURE 4). It also detected sodium (Na), magnesium (Mg), aluminum (Al), silicon (Si) and zinc (Zn) in or adjacent to the pigment layers, and in the ground at lower levels. Low levels of sodium, magnesium, aluminum, silicon, phosphorus (P), and titanium are all common in earth pigments. Zinc (in ZnO white pigment) can be seen in the EDS spectrum (FIGURE 5). Lead, Pb (from Pb pigments such as lead white) and barium, Ba (a component of lithopone) were not detected.

The element data are especially useful for constraining the time the painting was done. ZnO was known even in antiquity but was not synthesized in Europe until the 1780s. Opaque ZnO watercolor cakes were introduced by Winsor and Newton in 1834. Because ZnO makes oil films brittle and inhibits their drying, it was initially used only in watercolors (with gum binders). It was not until 1845 that the use of driers with ZnO in oils was commercialized, though ZnO still made paint films brittle. Although Zn was detected by EDS, its low level was not readily mapped, suggesting its presence might be from a later restoration. Finally, lead white was commonly used by Rembrandt and his Circle. However, it is not present in FIGURE 5.

Micro-Raman confirmed the presence of gypsum (1006 cm<sup>-1</sup>) and calcite (1084 cm<sup>-1</sup>). The varnish spectrum was consistent with dammar resin (30). A mix of hydrated iron oxides and small amounts of other pigments were also noted (31). The primer layer appeared to contain clay, but ZnO (438 cm<sup>-1</sup>) was not detected with certainty.

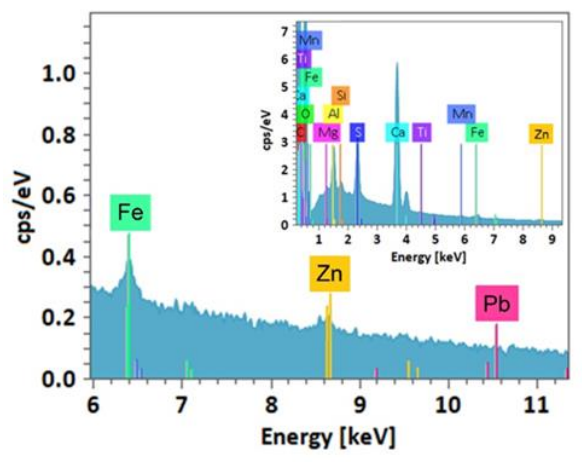


FIGURE 5 Spectrum of the major elements shown in the inset. The expanded scale shows zinc (Zn) at 8.64 keV, and no detectable lead (Pb) at 10.55 keV.

#### **Destructive methods**

Optional ICP-OES analyses

The SEM-EDS provides elemental analyses that map to locations at the micrometer scale in the paint chip, making it more useful than ICP-OES analyses. However, ICP-OES provides a bulk analysis and can detect lower levels of many elements. The relative percentages (by mass) of the elements in the pyrolysis char (see methods for *Exercise 6*) from a whole chip (gesso plus pigments, etc.) determined by ICP-OES were 2.1% aluminum, 0.1% barium, 95% calcium, 1.7% iron, 0.1% manganese,  $\leq$ 0.1% lead and 0.9% zinc. These confirm and help quantify the percentages of the pigments and gesso components detected by SEM-EDS. These elements are different from those reported to be in the *MGH-Original* (13), suggesting the *MGH-Copy* was not painted in the same studio at the same time.

#### Exercise 3A: Cross-section paint binder mapping

Paint cross-sections mounted in resin are partially destroyed in the process, as some of the material is lost. Once mounted, the range of analyses is more limited. However, this is a low-tech method for determining the structure of the paint film and many determinations can be conducted, both destructive and non-destructive. With optical microscopes, the sequence of paint layers can be observed. Many pigments and binding media may be identified with fluorescent and non-fluorescent stains. The sequence of fluorescent stains (FIGURE 6) and a negative starch test with KI/I<sub>2</sub> indicated a non-starch carbohydrate (e.g., a plant gum) and low levels of oil and protein in the *MGH-Copy* ground.

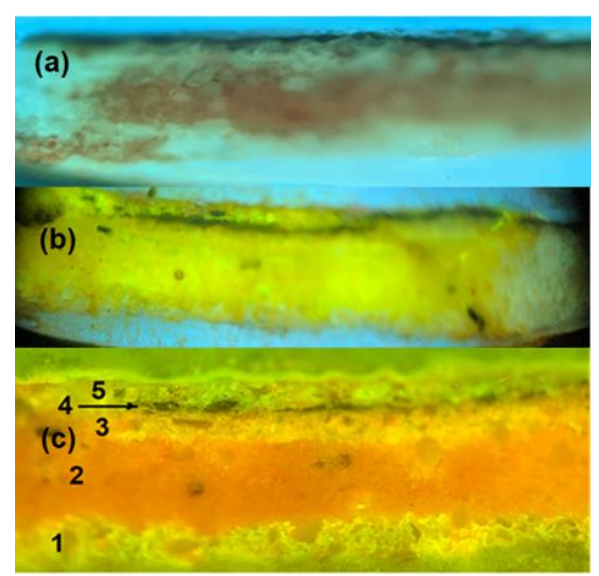


**FIGURE 6** Cross-section analyses of binding media using UV-VIS microscopy and color cubes to select excitation and emission wavelengths. (a) Red-brown stain with TTC was positive for reducing sugars (e.g., acacia gum); (b) yellow fluorescence with FITC was positive for proteins; and (c) Rhodamine-B red stain was positive for lipids after removing the excess with methanol. Foundation layer is (1), (2) is the ground, (3) is the primer layer, (4) is the pigment layer, and (5) is the varnish. Thickness = 0.3 mm

## Exercise 3B: Mapping of ZnO with dithizone

Zinc was deemed important for constraining the earliest date of the MGH-Copy. Therefore, an inexpensive, low-tech method for imaging zinc in the paint cross-section was sought to clarify the bulk SEM-EDS element data. The spot test of Plesters (22) used as a cross-section stain is inexpensive and gives a good image (FIGURE 7). The gypsum-calcite gesso provides a white, alkaline background for the green to red dithizone reaction with zinc. Although dithizone reacts with many metal ions, the only white pigments expected to react under these conditions are lead white, zinc white and lithopone (a barium sulfate, zinc oxide, and zinc sulfide mix). CaCO<sub>3</sub>, CaSO<sub>4</sub> and TiO<sub>2</sub> do not react. While 10% ZnO in gesso gives a red that persists for days, 10% lead white in gesso gives a pink that fades within hours.

In the MGH-Copy cross-section, the red stain appears in the upper portion of the ground (FIGURE 7) as well as in the pigment layer. This is important, as the presence of Zn in every chip tested suggests the ZnO is unlikely to be from a restoration. Finally, acacia gum was a binder for the watercolor pigment ZnO, and its distribution corresponds with where the ZnO is located. Due to ignorance or lack of access to ZnO powder or oil paint, the MGH-Copy painter appears to have used a watercolor

cake as a source of ZnO for the ground. While this is very unusual, as it will cause delamination of the paint, this explains the presence of carbohydrates in the analyses of the ground in **FIGURE 6.** 



**FIGURE 7** Dithizone stained ZnO on a fresh surface in the paint cross-section. The ZnO red stain correlated with the carbohydrate red-brown stain from TTC, suggesting a watercolor cake was used as a source of ZnO.

Exercise 4: Polarized light microscopy and microfossils

PLM and nannofossil analyses are not completely destructive, but separation of the binder from the particles is not reversible and the structure of the paint film is destroyed. However, only minute amounts of the sample are needed to identify many pigments. The morphology of the particles also offers insights into whether the particles are natural minerals that have been reduced to a powder or synthetic precipitates from reagent solutions.

The PLM analysis indicated the dark pigment particles were a mix of organic and inorganic particles based on their refractive indices and data from McCrone's Particle Atlas (32). Some of the dark particles floated to the top of the immersion oils over a period of days. This suggested the organic matter might be brown earth (lignite) found in traditional Van Dyke brown pigments. As some of it also dissolved, a synthetic Van Dyke brown pigment made from asphaltum/bitumen and hydrated iron oxides in the latter half of the 19<sup>th</sup> century is also possible. The denser dark particles were consistent with iron oxide pigments, in agreement with XRD and micro-Raman data. Most of the unpigmented particles' indices of refraction, based on their Becke line, oblique illumination, and contrast (33), were consistent with calcite and gypsum.

Micropaleontology has been in use for many decades to identify geologic formations, and the diatom test for drowning cases is well known (34). Just as major fossil species varied over time, latitude, and environmental conditions, so did nannofossils. Nannofossil analyses in materials important to cultural heritage, such as chalk and clay, are emerging as tools for answering questions of authenticity and provenance (35-36).

While microfossils (e.g., diatoms) are observable with standard magnifications (100–500x) used for PLM analyses, nannofossil identification routinely uses 1000x with verification of species-level detail via SEM. The time needed for sample preparation, analysis, and identification of multiple species currently limits this exercise to small undergraduate or graduate courses. However, advances in SEM technology and AI are

lowering this barrier (34). As forensic scientists usually rely on expert microscopists, "reports" are provided to lower-level classes instead.

Diatoms typically fall between 20  $\mu$ m and 200  $\mu$ m while nannofossils vary between 0.3  $\mu$ m and 30  $\mu$ m. However, even 500x with crossed polarizers can detect some nannofossils like the cubic *Micula* species (37). A thin (#0) coverslip is used with the 100x oil immersion lens due to the small depth of field at high magnification.

Calcareous nannofossils have crystalline skeletons. Many have distinctive "Maltese Crosses" when viewed with crossed polarizers. However, starch grains can look similar. Therefore, particle morphology should be observed without crossed polarizers if starch is present. Starch grains are rounded (32), while nannofossils observed in this study were small cubes (37). Diatoms from the Rocky Mountains were also identified, but these were attributed to recent dust contamination.

The nannofossils tentatively identified with the PLM microscope were Micula staurophora (synonym for M. decussata) (37). These nannofossils are from the Late Cretaceous (66-90 Mya). M. staurophora are abundant in the Campanian and Maastrichtian formations, which are named after the chalk formations in Champagne, France and Maastricht, the Netherlands. These formations are consistent with the provenance of chalk used by Rembrandt's Circle. However, French chalk was being sold to artists all over the world by 1800. Furthermore, Micula staurophora is found in other Late Cretaceous formations, including in Italy and Argentina. A profile of different nannofossils species is needed to specify a geolocation, and source use over time should be taken into consideration when applying this method due to strata variation.

#### Exercise 5: Paint film oil date

The literature reports various methods for preparing small paint samples for the analysis of oil binders, usually after conversion to FAMEs, as these are much more volatile than the parent triglycerides or acids. Different pigments and their concentrations affect the initial drying rate (38). These effects tend to average out in mixtures. Similar approaches may be used for proteinaceous binders (39) The FAME ratios from fresh lipid binders vary with the oil source. Sometimes these differences (especially the lower concentration FAMEs) are used to identify the oil, though there is a great deal of overlap between oils.

Unsaturated fatty acids (FAs) oxidize or polymerize faster than saturated FAs. The saturated FAs are more stable and are used for oil identification. If a single source (e.g., linseed oil) is assumed, the ratios of the unsaturated FAs may be used to obtain an approximate date for when a painting was done. In the MGH-Copy, the ratio of palmitic (C16:0) to stearic (C18:0) acid (P/S) = 2.75. This

fits walnut oil with P/S = 2-4.5, or egg P/S = 2.3-4.3. The rate of polymerization and oxidation depends on variables like light levels, pigments, and lipid profiles: oil dates are only rough estimates (40). To a first approximation the residual monounsaturated C18:1, compared to dated linseed and walnut oil paint samples plotted in **FIGURE** 8 suggests the painting was produced ca.  $1892 \pm 16$  (1s) CE, a date in agreement with the 1898 showing of the *MGH-Original*.

#### Oil Age Calibration

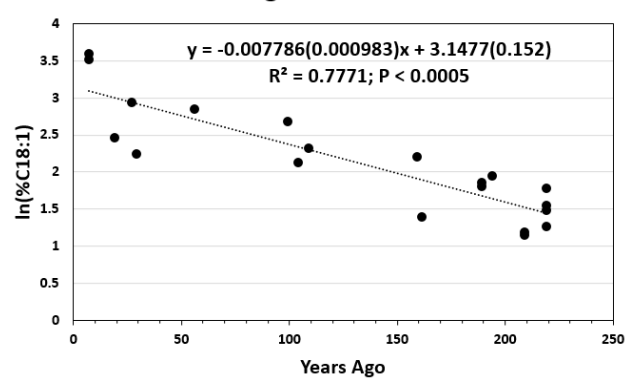


**FIGURE 8** Calibration data for approximate dating of linseed and walnut oils.

Exercise 6: Identification of paint binders and pigments using Py-GC-MS

An estimate of the organic components from a sample may be obtained by Py-GC-MS. This direct method offers advantages and disadvantages compared to the analysis after derivatization (41). Derivatization provides lower detection limits for selected components while pyrolysis gives a simultaneous analysis of all the components. Because complex chromatograms are created, commercial instruments provide temperature programmed pyrolysis.

**FIGURE 9** shows the TIC (total ion chromatogram) obtained from the off-line, vacuum pyrolysis of a 1.5 mg chip from the *MGH-Copy*. Furans suggest the presence of carbohydrates, nitrogenous compounds imply proteins, fatty acids and linear hydrocarbons indicate oils, and resins and tars create polyaromatic hydrocarbons (PAHs). A single analysis of the limited sample provided insights into the various organic components (42).

The *MGH-Copy* pyrogram (**FIGURE 9**) provided evidence for coal tar (many PAHs) and pine resins (longifolene, retention time, RT = 15.80, retention index, RI = 1405, and retene, RT = 26.76, RI = 2244). It indicated the presence of lipids (e.g., methyl palmitate, RT = 23.07, RI = 19.33) and carbohydrates (furans) in the MGH-Copy.

Even without derivatization, the pyrolysis formed small amounts of 2,5-diketopiperazines from

combinations of amino acids from the protein binder. These were identified with SIM (selective ion monitoring) from their retention indices and unique mass fragments (43). Cyclo-(Pro-Pro) and cyclo-(Pro-Gly) were identified in rabbit skin glue-gesso and casein-gesso exemplar mixtures and in the *MGH-Copy*.

Glycine makes up ca. 25% of collagen versus 2.5% of casein. The ratio of cyclo-(Pro-Gly) (RT = 20.86, RI = 1760) to cyclo-(Pro-Pro) (RT = 23.25, RI = 19.47) in the MGH-Copy = 3.45. This fits with the ratio for gelatin

(3.2) from collagen. For collagen or rabbit skin glue pyrolyzed with gesso, this drops to 1.3-1.8; in caseingesso it is  $\leq 0.1$ ; and in whole egg  $\leq 0.7$ . These data suggest purified collagen or hide glue was used in the MGH-Copy, not casein, milk, or egg binder (39). Nor was cholesterol (a marker for egg binders) detected in the MGH-Copy, though other animal steroids were detected. Eggs also have lower total levels of glycine and proline than hide glues. Based on collagen standards, the MGH-Copy paint chip contained 1.5-2% collagen.

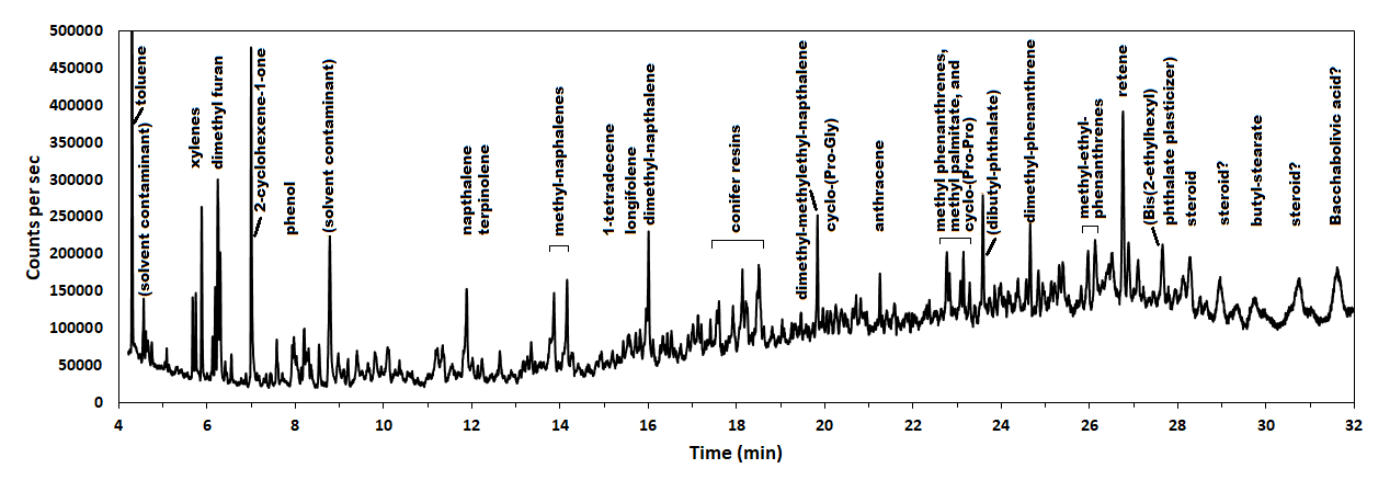


**FIGURE 9** Pyrogram of a 1.5 mg chip from *MGH-Copy*. Most furans eluted in the first 10 min, and lipid esters, protein degradation products, and resin products between 15 and 30 min. Some components hint at a South American plant origin and a provenance. The many naphthalene, etc. compounds suggest a coal tar or brown coal Van Dyke brown pigment.

#### **Conclusions**

The dimensions of the wood panel and image placement (including cropping of the feathers) replicate those of the canvas painting in Berlin, suggesting 1796 as the *MGH-Copy*'s earliest date. The radiocarbon date is also too recent for Rembrandt. The *MGH-Original* was not shown publicly until 1898, and a photogravure did not appear until 1907. The copy appears to be painted on an earlier, recycled wood panel, maybe from Argentina from ca. 1820. It was stained to appear old. Furthermore, some of the plant resins, the presence of ZnO watercolor pigment in the primer layer, and the oil date, even with their uncertainties, suggest the *MGH-Copy* was likely painted ca. 1900 in South America.

The exercises include most of the methods listed for forensic paint analysis by the American Society of Trace Evidence Examiners (44). The limited sample emphasized the value of careful planning of a sequence of analyses. The analyses were able to estimate the date of production, composition, varnish, pigments, and binders, and they provided insights into the artist's technique. By using a sequence of analyses that began with non-destructive methods and progressed to minimally invasive techniques, the amount of information obtained was

maximized. The sequence provided cross-validation with enough detail for a provenience reconstruction that mimics the thought processes involved in crime scene reconstructions.

#### Acknowledgments

We thank Lawrence Kaplan and Patricia Hill for their NSF-CWCS forensic science and art-chemistry courses, and Colorado College for a Creativity and Innovation Grant. We also thank the Otis and Margaret Barnes Trust for grants that supported the purchase of the ATR-FTIR, GC-MS, and XRD. Raman measurements were supported by the National Science Foundation Major Research Instrumentation award #2117144.

#### References

- Durrani A. Taking on art fraud. Plaintiff 2011 Jan:1-20. https://www.plaintiffmagazine.com/recentissues/item/taking-on-art-fraud (accessed Jan 11, 2023).
- 2. Houck M, Smith GD. The forensic mindset: art and crime. Forensic Sci Int: Synergy 2021;3:100143.

- 3. Tiligadas M. Stealing beauty: The history of art forgery, and the rise in art thefts during the pandemic. The Science Survey, News. Feb 2022;1. https://thesciencesurvey.com/news/2022/02/01/stealing-beauty-the-history-of-art-forgery-and-the-rise-in-art-thefts-during-the-pandemic (accessed Jan 11, 2023).
- Art News. Over 50 percent of art is fake. Art News Oct 13, 2014; Galleries. https://news.artnet.com/market/over-50-percent-of-artis-fake-130821 (accessed Jan 11, 2023).
- 5. Kaye LM, Spiegler HN, Weitz YM, Wilson GC. The art law review: USA. The Law Reviews 2023;Jan 6. https://thelawreviews.co.uk/title/the-art-law-review/usa (accessed Jan 11, 2023).
- 6. Miranda MD. The trace in the technique: Forensic science and the Connoisseur's gaze. Forensic Sci Int: Synergy 2021;3:100203.
- 7. Quarino L, Brettell TS. Current issues in forensic science education. Anal Bioanal Chem 2009; 394(8):1987-93.
- 8. Harmon KJ, Miller LM, Millard JT. Crime scene investigation in the art world: The case of the missing masterpiece. J Chem Educ 2009;86(7):817-9.
- 9. Brasuel MG, McCarter AD, Bower NW. Forensic art analysis using novel reflectance spectroscopy and pyrolysis gas chromatography mass spectrometry instrumentation. Chem Educator 2009;14(4):150-4.
- 10. Wells G, Haaf M. Investigating art objects through collaborative student research projects in an undergraduate chemistry and art course. J Chem Educ 2013;90(12):1616-21.
- 11. Nielsen SE, Scaffidi JP, Yezierski EJ. Detecting art forgeries: A problem-based Raman spectroscopy lab. J Chem Educ 2014;91(3):446-450.
- 12. Fieberg JE, Smith GD. Dry laboratory forgery investigation of a purported Giorgio de Chirico painting for a "Chemistry in Art" course. In: Contextualizing Chemistry in Art and Archaeology: Inspiration for Instructors. ACS Symposium Series 1386, 2021; Chap. 13:315-56.
- The Rembrandt Database. Provenance, circle of Rembrandt, The man with the golden helmet, c. 1650. Gemäldegalerie (Staatliche Museen zu Berlin), cat. 811A. https://rkd.nl/explore/images/202398 (accessed Jan 11, 2023).

- 14. Stuart BH. Analytical Techniques in Materials Conservation, Chichester, UK:Wiley. 2007.
- Doménech- Carbó MT, Osete-Cortina L. Another beauty of analytical chemistry: chemical analysis of inorganic pigments of art and archaeological objects. ChemTexts 2016;2(14):1-50.
- 16. Craddock P. Scientific Investigation of Copies, Fakes and Forgeries. New York, Elsevier 2009.
- 17. Tomak ED, Ustaomer D, Yildiz S, Pesman E. Changes in surface and mechanical properties of heat-treated wood during natural weathering. Measurement 2014; 53:30–9.
- Petrillo M, Sandak J, Grossi P, Sandak A. Chemical and appearance changes of wood due to artificial weathering – Dose–response model. J Near Infrared Spectrosc 2019;27(1):26–37.
- Sandu ICA, Schäfer S, Magrini D, Bracci S, Roque CA. Cross-section and staining-based techniques for investigating organic materials in painted and polychrome works of art: A review. Microsc Microanal 2012;18:860–75.
- 20. Wolbers R, Landrey G. The use of direct reactive fluorescent dyes for the characterization of binding media in cross-sectional examinations. 15th annual meeting of the American Institute for Conservation of Historic and Artistic Works. Vancouver, BC, Canada, May 20-24, 1987 168-204. https://www.wagaic.org/1987/wolbers-landrey87.pdf (accessed Jan 26, 2023).
- 21. Doménech-Carbó MT, Doménech- Carbó A. Spot tests: past and present. ChemTexts 2022;8(4):1-66.
- 22. Plesters J. Cross-sections and chemical analysis of paint samples. Stud Conserv 1956;2(3):110-57.
- 23. EUR-Lex. Commission implementing regulation (EU) 2015/1833 of 12 October 2015 amending regulation (EEC) No 2568/91 on the characteristics of olive oil and olive-residue oil and on the relevant methods of analysis. http://data.europa.eu/eli/reg\_impl/2015/1833/oj (accessed Jun 1, 2022).
- 24. Bower NW, Blanchet CJK. Analytical pyrolysis-chromatography: Something old, something new. J Chem Educ 2010;87(5):467-9.

- 25. Thoury M, Elias,M, Frigerio J-M, Barthou C. Nondestructive varnish identification by ultraviolet fluorescence spectroscopy. Appl Spectrosc 2007; 61(12):1275-82.
- 26. Cosentino A. Identification of pigments by multispectral imaging; a flowchart method. Herit Sci 2014;2(8):1-12.
- 27. Shin J, Choi S, Yang JS, Song J, Choi JS, Jung HI. Smart Forensic Phone: Colorimetric analysis of a bloodstain for age estimation using a smartphone. Sens Actuators B 2017;243:221–5.
- 28. Belenki L, Sterzik V, Schulz K, Bohnert M. Analyzing reflectance spectra of human skin in legal medicine. J Biomed Opt 2013;18(1):017004.
- 29. Mayer L. Myers G. A note on the early use of dammar varnish. Stud Conserv 2002; 47(2):134-8.
- 30. Daher C, Paris C, Ho ASL, Bellot-Gurleta L, Echard, JP. A joint use of Raman and infrared spectroscopies for the identification of natural organic media used in ancient varnishes. J Raman Spectrosc 2010;41:1494–9.
- 31. Bell IM, Clark RJH, Gibbs PJ. Raman spectroscopic library of natural and synthetic pigments (pre- ≈ 1850 AD). Spectrochim Acta A 1997;53(12):2159–79.
- 32. McCrone WC, Draftz RG, Delly JG. The Particle Atlas, 2nd Ed., Ann Arbor (MI): Ann Arbor Science Publishers Inc., Vol. 1-4, 1973, Vol. 5, 1979, Vol. 6, 1980. (See pp. 810–837; 1399–1401; and 1402–1413). Although out of print, online resources are available at: https://www.mccrone.com/mm/resources-for-paint-pigment-microscopists/, including a free reprint of "The Microscopical Identification of Artists' Pigments" by Walter C. McCrone.
- 33. Chamot EM, Mason CW. Handbook of Chemical Microscopy, 3rd ed., vol. 1, New York: Wiley 1958: 314-8.
- 34. Zhou Y, Cao Y, Huang J, Deng K, Mae K, et al (9). Research advances in forensic diatom testing. Forensic Sci Res 2020; 5(2):98–105.
- 35. Fiorentino A. The potential of nannofossil analysis applied to archaeological studies: The case of the Riace's Bronzes. J Nannoplankton Res 1998; 20(2):101–3.

- 36. Kędzierski M, Kruk MP. Similarity and provenance of underpainting chalk grounds based on their nannofossil assemblages cluster analysis. J Cult Herit 2018;34:13–22.
- 37. Young JR, Bown PR, Lees JA. Nannotax3 website. Intl Nannoplankton Assoc. 2023. www.mikrotax.org/Nannotax3 and https://mikrotax.org/Nannotax3/index.php?id=10683 (accessed Jan 11, 2023).
- 38. Tammekivi ES, Vilbaste VM, Leito I. Quantitative GC–MS analysis of artificially aged paints with variable pigment and linseed oil Rratios. Molecules 2021;26:2218, 1-13.
- 39. Chiavari G, Lanterna G, Luca C, Matteini M, Prati S, Sandu CA. Analysis of proteinaceous binders by insitu pyrolysis and silylation. chromatographia 2003; 57(9/10):645–8.
- 40. Bonaduce I, Carlyle L, Colombini MP, Duce C, Ferrari et al (8). New insights into the ageing of linseed oil paint binder: A qualitative and quantitative analytical study. PLoS ONE 2012;7(11):e49333.
- 41. Colombini MP, Modugno F, Ribechini E. GC/MS in the characterization of lipids. In: Colombini, M, Modugno, F, editors. Organic Mass Spectrometry in Art and Archaeology. Chichester, UK: Wiley, 2009.
- 42. Ghelardi E, Degano I, Colombini PE, Mazurek J, Schilling M, Learner T. Py-GC/MS applied to the analysis of synthetic organic pigments: characterization and identification in paint samples. Anal Bioanal Chem 2015;407:1415–31.
- 43. Fabbri D, Adamiano A, Falini G, De Marco R, Mancini I. Analytical pyrolysis of dipeptides containing proline and amino acids with polar side chains. Novel 2,5-diketopiperazine markers in the pyrolysates of proteins. J Anal Appl Pyrolysis 2012;95:145–55.
- 44. American Society of Trace Evidence Examiners, Scientific Working Group for Materials Analysis, Paint Subgroup: Forensic Paint Analysis and Comparison Guidelines, 2000. https://www.asteetrace.org/swgmat.



https://creativecommons.org/licenses/by-nc-sa/4.0/legalcode. This work is licensed under Creative Commons license BY-NC-SA 4.0.